

On the dynamics and spreading pathway of the Persian Gulf outflow

A. A. Bidokhti¹ and Ezam²

¹Institute of Geophysics, University of Tehran, P. O. Box: 14155-6466, Tehran, Iran.

²IAU, Science and Research Center, Tehran, Iran.

*E-mail of presenting author: Bidokhti@ut.ac.ir

Abstract: Results of numerical simulation and some observational data are used to study the Persian Gulf outflow structure and its spreading pathways during two different time of the year, mid-winter and early summer. The results reveal that during the winter the outflow boundary current detaches from the coast well before the Ras Al Hamra Cape, however for the summer the outflow seems to follow the coast even after this Cape at shallower depth. This is due to higher density of the outflow due to lower temperature that leads to more sinking of the outflow during the winter. Thus, it moves to deeper parts at about 300-400 m in contrast with that of summer which is at about 200-300 m. During winter, the deeper, stronger and wider outflow is more affected by the steep topography, leading to separation from the coast. While during summer weaker and shallower outflow, is less influenced by the bottom topography and seems to disappear downstream of the Ras Al Hamra Cape.

Keywords Outflow, Persian Gulf, Spreading pathways.

1. Introduction

The Persian Gulf is a semi-enclosed marginal sea which is connected to the Indian Ocean through the Strait of Hormuz and the Oman Sea. High evaporation rate between $1.5\text{--}2\text{ m yr}^{-1}$ and the shallowness of the Persian Gulf especially in vicinity of southern coasts leads to formation of saline and dense water with maximum salinities up to about 57 in shallow estuaries along the southern coasts (John and Olson, 1990), although the maximum salinity range over most of the Persian Gulf is about 40.0-40.5 (Brewer et al., 1978). Most saline water in the Persian Gulf is observed during the first half of year compared to second half (Bower et al., 2000; Johns, 1998), and it is cooler by several degrees during February-June compared to July-January. The saline water sinks to the deeper zone due to higher density and form a density front. The dense water exits the Persian Gulf through the Strait of Hormuz as a bottom boundary current, banked against southern coasts, and fresher Indian Ocean water enters the Persian Gulf as a surface current mostly on the northern side (Brewer et al., 1978; Swift and Bower, 2003).

Here we use some observations and numerical modeling to consider the Persian Gulf outflow. The numerical simulations are performed at two different times of the year (mid winter and early summer), when the CTD

measurements are available and are utilized to bring about buoyancy forcing at the western boundary of the model domain. In addition, surface wind fields are prepared from averaged monthly wind over the model domain.

2. Some Observational data

Hydrographic measurements are those of the ROPME expedition in 1992 (Reynolds, 1993). The CTD measurements collected in this expedition are the only comprehensive ones and therefore are appropriate for this study. In addition, data were collected at two different times of the year and so the temporal variability of the outflow can be considered to some extent.

Fig. 1 shows the CTD transects along the axis of the outflow for winter and summer. It is clear that in winter

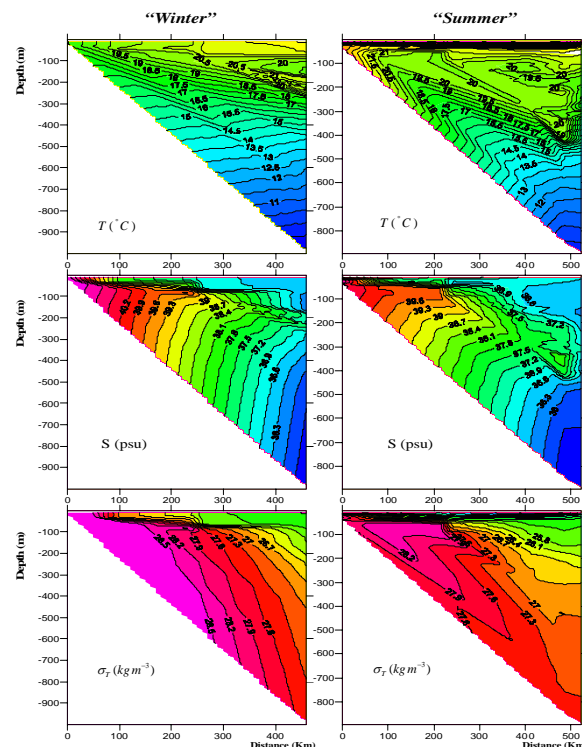


Fig. 1 CTD measurements along the outflow paths for winter (Feb.) (left) and summer (May)(right)

the outflow is colder and extends to deeper parts than the summer one. Fig. 2 also shows the variations of T and S along the outflow axis, indicating that the salinity change

is very small between the two seasons while the temperature difference is large. This indicates that the annual variation of temperature seem to cause the density change between the two seasons.

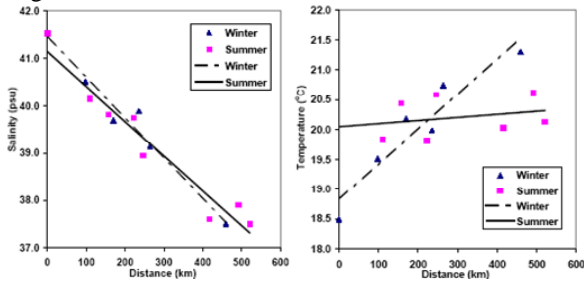


Fig. 2 Salinity and temperature variations of the outflow along the axis of the outflow to the open sea for winter and summer.

3. The numerical model

The numerical model namely, Princeton Ocean Model is set up by CTD measurements at its western boundary and monthly surface wind speed on the model domain (Fig. 3) from ICAODS data. The model uses the mode splitting technique which is the separation of fast moving surface gravity waves in 2D barotropic mode and solving them using high order explicit finite difference methods with external time step, from the slower moving one in 3D baroclinic mode and solving them implicitly with internal time step. Here the ratio of internal to external time step is chosen as 60 (Ezer, et. al., 2002).

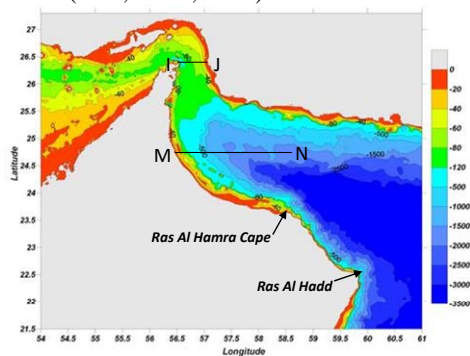


Fig. 3: Model domain and topography including east of Persian Gulf and Oman Sea

The vertical mixing coefficients in the model are calculated by a second order turbulence closure model, namely Mellor-Yamada level 2.5 model (1982) of turbulence that is characterized by two quantities, turbulence kinetic energy and turbulent length scale. The horizontal diffusion in the model is also calculated from Smagorinsky scheme. The horizontal grid resolutions are approximately 3.5 km and we employed 32 vertical layers with logarithmic distribution in order to better represent the surface and bottom boundary layers. Initial temperature and salinity of the model domain were extracted from WOA05, which contains global monthly and annual

temperature and salinity with one and one forth degree resolutions. The amplitudes and phase speeds of the four major tidal constituents (M2, S2, O1 and K1) were prescribed at the open boundaries from the Admiralty Tide Table and assumed as constant along the boundaries.

4. Results and discussion

The model was initialized from initial conditions and was integrated for 10 successive years with implementation of monthly varying forcing at the surface and lateral boundaries until a quasi steady state was reached. The time series of domain averaged temperature and salinity for the last 6 years of integrations are shown in Fig. 4. All the time series have been plotted after taking the moving averaged with 15 days intervals to filter the tidal and higher frequency changes. Here, the results of the last year of integrations are presented.

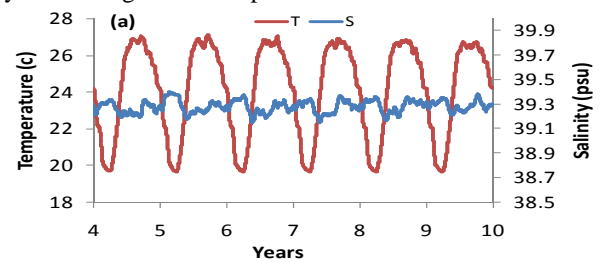


Fig. 4 Temperature and salinity variations for the last 6 years of simulations.

Fig. 5 shows the mean monthly temperature, salinity and sigma-T and two components of current along transect I-J across the Hurmoz Strait for March and August. In March, the temperature shows a nearly homogenous structure as the one inside the Persian Gulf, and the source of the outflow is indicated by the water mass with salinity more than ~ 39 psu and temperature of $\sim 19.5^\circ\text{C}$. In Aug., the vertical temperature differences up to 10°C are observed. The outflow is indicated by salinity more than ~ 39 psu, while its temperature varies between 24 and 26°C . Hence, the mean outflow sigma-T varies from about 28.1kgm^{-3} during March to about 26kgm^{-3} during Aug., which is mainly as the results of outflow temperature variations by more than about 6°C . The maximum volume transport of the PG outflow occurs during Feb-March (about 0.57 Sv) and it reaches to its minimum during Nov. (about 0.23 Sv) with a mean annual of about 0.35 Sv at the transect I-J. The simulation results are consistent with finding of Bidokhti and Ezam (2009) but are more than findings of Johns and Olson (1998) that suggested annual mean of 0.2 - 0.25 Sv for the PG outflow transport. It may be due to the fact that we estimated the PG volume transport at the entrance to the Oman Sea where dilution could have increased the volume transport. Bower et al. (2000) have estimated the dilution of the Persian Gulf water to the Oman Sea by factor of ~ 4 .

During March (winter months) a two layer density regime is observed, namely an upper layer with sigma-T of about 26kgm^{-3} and lower layer with sigma-T values more than

28.5 kgm⁻³. However, During Aug., (summer months) three layer stratification is observed, namely an upper low density layer with sigma-T of about 23kgm⁻³, the intermediate layer with a value of about 25.5kgm⁻³ and lower layer with a value of about 27kgm⁻³. It can be concluded from these values that during March higher density differences between benthic layer and upper layer (about 2.5 kgm⁻³) leads to higher stratification and therefore the entrainment and mixing between the outflow and upper layer decreases in comparison with Aug. in which the density difference is weaker in water column (about 1.5 kgm⁻³). The stronger and thicker outflow density in March (winter) leads to higher outflow velocity and volume transport in contrast to Aug. (summer).

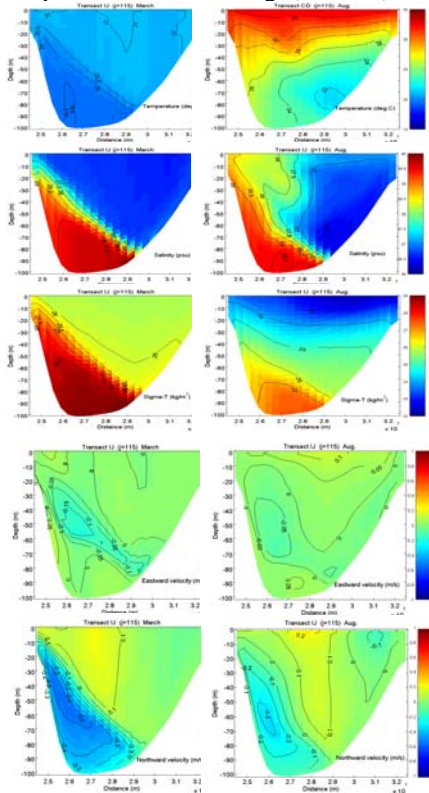


Fig. 5: Cross-section of the mean temperature, salinity, sigma-T and mean velocity components (east and north wards) at the Strait of Hormuz (I-J) obtained from model simulation during March (left) and August (right)

The mean monthly velocity components across the Strait (Fig. 5) exhibit the highest velocities at depths of 30-70 m with more than 0.5 ms⁻¹ in March, and at depths of 50-70 m with velocity of about 0.3 ms⁻¹ in August. The direction of the outflow at these depths is mainly southward. The westward component of the flow can be due to thermal wind effects that cause the flow to turn right with height. The denser outflow source water in March, and also lesser entrainment and mixing in comparison with Aug., lead to the outflow intrusion into the deeper equilibrium depths. Thus, the equilibrated outflow is observed with mean depths of 200 m and down to 400 m during Aug. and

March respectively (Figs. 6). The sigma-T transects (not shown) also confirm that the outflow has reached its equilibrium levels. The lower source density of the outflow during Aug. causes it to mainly appear in the shallower zone relative to that of March. Hence, in Aug. the outflow is more evident at the depth of 200 m and propagates as a narrow boundary current in vicinity of southern and western coasts, disappearing downstream of the the Ras Al Hamra Cape located at 58.5 °E and 23.8°N(Fig. 7).

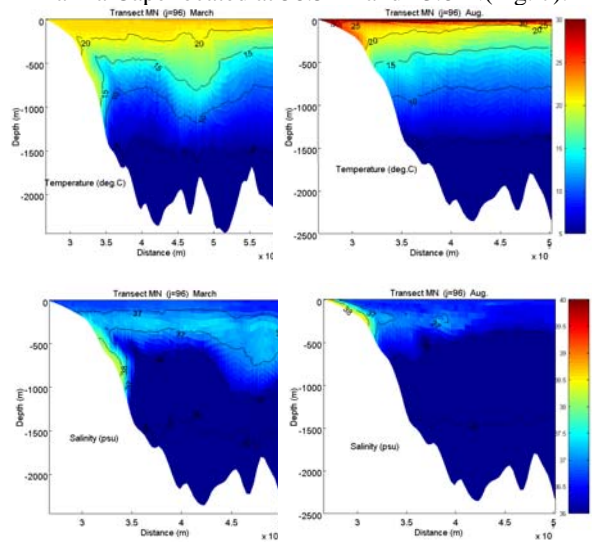


Fig. 6: Cross-section of the mean temperature and salinity along MN path, shown in Fig. 3 obtained from model simulation during March (left) and August (right)

As a whole, it could be concluded that during Aug., the low outflow density and volume flux, with eddy activities in the region are the main reasons that the outflow disappears after the Ras Al Hamra Cape. Also, the advections of the outflow water by eddies cause it to appear far away from its main branch, even in central and northern parts of the Oman Sea. On the other hand, in March the major part of the outflow which is colder and saltier descends rapidly on the continental slope before mainly being affected by eddies in the upper layers of the Oman Sea, and finally, it reaches the equilibrium depth of about 400m. At this time, the outflow propagates as a boundary current like that of Aug., until it approaches the 58 °E – 24 °N near the Cape of Ras Al Hamra. Here, it detaches from the lateral boundary and moves east and then north-east meanwhile a relatively weak cyclonic circulation is observed on its left side (as observed in the upper layers) that contain less outflow water characteristics. Finally, at the end of its path, an anti-cyclonic eddy is formed that carries more outflow features. The Peddy (Persian Gulf eddy) contains the temperature and salinity of the outflow. Senjyu, et al. (1998) suggested that the formation of the Peddy is related to the intermittency of outflow movement through the Strait of Hormuz.

We also performed the simulation without including the tide. The results show that separation of the outflow from lateral boundary occurs as before. But the outflow spreads as an "S" shape meander in winter while moving along the coast in summer (Fig. 8). These Figs. show the horizontal field of the salinity and their corresponding velocities at depths 300m. It can be deduced from the figures that the outflow during May mainly appears in the shallower zone relative to that of February because of its lower density. So during May, the outflow that is more evident at the depth of 300 m continues its propagation as a narrow boundary current in vicinity of southern and western coasts. After passing the Ras Al Hamra Cape the outflow widens in width as observed by Pous et.al (2004), while it loses its heat and salinity owing to mixing with ambient water. When it reaches the Ras Al Hadd region (located at 59.7 °E and 25.5 °N) it turns to offshore (east) and acquires a cyclonic circulation. In February the main part of the outflow reaches the deeper depths (500m) and propagates as a boundary current until it reaches the Ras Al Hamra Cape, where it detaches from the coast (as also seen in Fig. 7) and moves northward and then turns east while flowing along the isobaths of 500 m and forms an "S" shape meander. On the left side of the meander a relatively weak cyclonic circulation is formed that contain less outflow water characteristics. While on its right side a more intense anti-cyclonic eddy forms that carries more outflow features. Another small portion of the outflow still continues its motion as a boundary current until it reaches the Ras Al Hadd Cape. Here it turns right (east) as in May and forms a cyclonic eddy. We found that this cyclonic circulation has a permanent existence during both months at the place where the outflow water meets the Indian Ocean inflow water (Ras Al Hadd Cape) and possibly the Cape effect can contribute to its formation (as mentioned by Tao (1987); Asaro (1998); Pous, et. al. (2004)). Maybe during May the commencing of Monsoon wind could contribute to intensify this circulation and causes it to appear on the surface as well.

Stern (1980) showed that for a coastal gravity current with zero potential vorticity assumption, if the current width far upstream of the nose is less than a critical fraction (0.42) of the Rossby radius of deformation (based on the current depth far upstream), then the nose of the current will propagate along the coast as a bore and the form of the nose may be steady if the friction is able to dissipate sufficient kinetic energy.

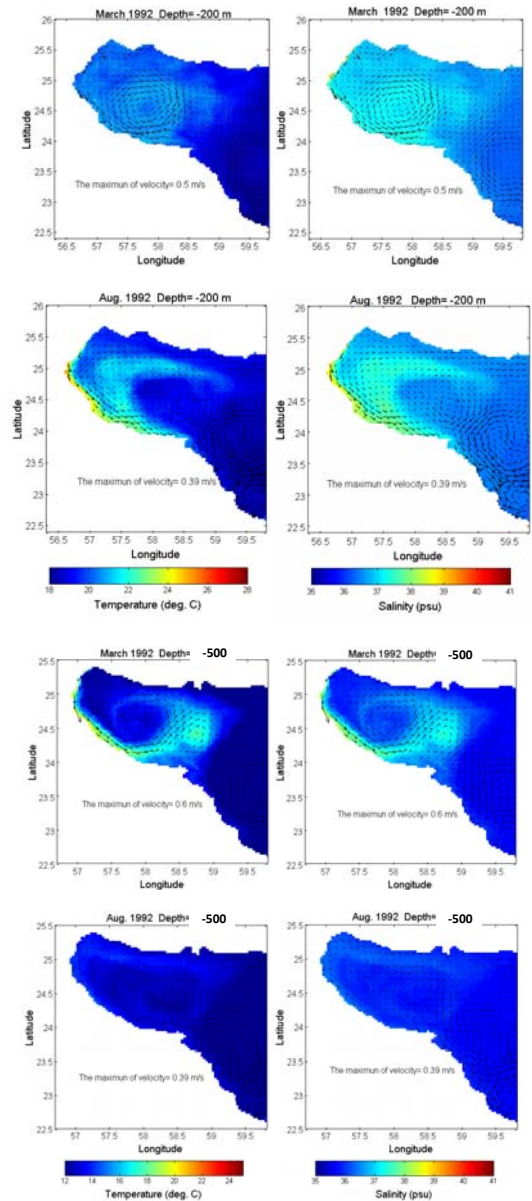


Fig. 7: Horizontal mean fields of temperature and salinity at depth 200m for March and 500m for August.

However, if the upstream current is wider than this critical value, the flow may be blocked and deflected perpendicular to the coast. We implemented the Stern theory (however the outflow vorticity may not be zero) to assume the different behavior of the outflow near the Ras al Hamra Cape.

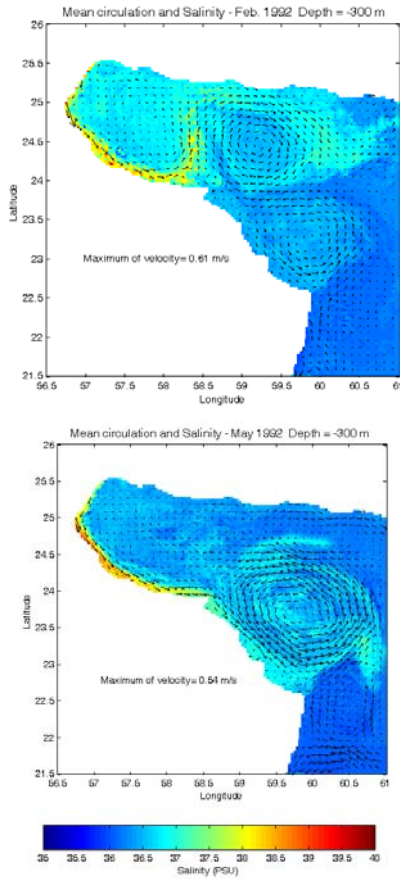


Fig. 8: Horizontal salinity field at depth 300m for February (top) and May (below)

Extracting the outflow characteristics at a place some before the Cape yields: $h \sim 400, 200$ m (outflow depth); $g' \sim 0.015, 0.012 \text{ ms}^{-2}$ (reduced gravity), $W \sim 40, 10$ km (outflow width) and $f \sim 6.0 \times 10^{-5} \text{ s}^{-1}$ (Coriolis parameter) for March and Aug. respectively. Therefore, the corresponding Rossby radius of deformation ($\sqrt{g'h}/f$), are approximately equal to 46 and 24 km for March and Aug respectively, that lead to critical current widths of order of 19 km for March and 11 km for Aug. Comparing these values with outflow widths, it could be concluded that during March the outflow should detach from the coast and propagate normal to the coast, while during Aug. it should continue its propagation along the coastal boundary (as seen in Fig. 8). An additional explanation for the separation and Peddy formation is that during March, as PG the outflow moves to deeper zone of the Oman Sea, encountering the steep topography near the Ras al Hamra Cape (as seen in Fig. 1), the outflow thickness increases (due to stretching processes) and so the compression of water column above and below it take places. Therefore, due to conservation of the potential vorticity an anti-cyclonic circulation may be introduced above the outflow intrusion (as speculated by Junglaus, 1999).

5. Conclusions

The model simulations showed nearly good agreement with measurements in 1992. The simulation revealed that the mean salinity of the PG outflow source water is almost constant (~ 39 psu, with an annual variation of about 0.2 psu) during the whole year but its mean temperature shows an annual cycle and varies between 19 and 27 °C. These lead to the variations in the outflow density of order of 2 kgm^{-3} during the year. The maximum and minimum densities of the outflow occur during late winter (March) and midsummer (August) respectively. The highest density of the outflow source water causes it to penetrate to the deeper depths in the Oman Sea during March.

The simulations showed the appearance of the outflow down to 400 m during March as a boundary current banked against western continental slope while it spreads laterally at mid-depths of about 250 m due to eddy activities. In some previous literatures (e.g. Senjyu et al., 1998; Matsuyama, et al. 1998; Bower, et al., 2000; Pous et al., 2004) the mean depth of the outflow spreading in the Oman Sea has been found to be at about 250-400m. Our simulations are nearly consistence with the measurements of Senjyu et al. (1998), which have been made during January 1994, and the measurements of the Pous et al. (2004), during October and early November 1999. Accordingly, winter cooling of the surface in the Persian Gulf enhances the outflow density, hence, the deeper equilibrium depth of the outflow in the late winter (March) maybe expected. During the summer the outflow has a lower source density, hence it spreads into the shallower depths near the coastal boundaries. During March (winter) the outflow with higher density spreads into the deeper parts and separate from the lateral boundary as it approaches the Ras al Hamra Cape, and effects as larger width of the outflow, steep topography and tidal oscillations appear to generate the Peddy.

It is also worth mentioning that the double diffusion convection along the bottom part of the outflow can be very effective in reducing the outflow density (by downward mass flux) and this effect is not included in the simulation which shows a larger sinking of the outflow, especially in winter. In future work this factor should be included in such simulation.

As a whole, we find that the seasonal variations of the outflow source water characteristics lead to different outflow pathways in the Oman Sea. The outflow is affected by different mechanisms in the Strait of Hormuz and the Oman Sea such as vertical mixing due to interaction by tide that leads to intermittency in outflow moving into the Oman Sea. The short time variability of the outflow and other dynamical processes such as barotropic and baroclinic instabilities can lead to the outflow intermittency and as a result eddy generations in the Oman Sea which is not considered in the present work.

References

1. Bidokhti, A. A. and Ezam, M.: The structure of Persian Gulf outflow subjected to density variations, *Ocean Science*, 5, 1-12, 2009.
2. Bower, A. S., Armi, L. and Ambar, I.: Lagrangian observations of meddy formation during a Mediterranean Undercurrent seeding experiment, *Journal of Physical Oceanography*, 2545–2575, 1997.
3. Bower, A. S., Hunt, H. D. and Price, J. F.: Character and dynamics of the Red Sea and Persian Gulf outflow, *J. Geophys. Res.*, 105(C3): 6387-6414, 2000.
4. Ezer, T., Arango, H. and Shchepetkin, A. Developments in terrain-following ocean models: intercomparisons of numerical aspects. *Ocean Modelling* 4 (2002) 249–267
5. Jungclaus, J. H.: A three dimensional simulation of the formation of anticyclonic lenses (meddies) by the instability of an intermediate depth boundary current, *J. Phys. Oceanogr.*, 29, 1579-1598, 1999.
6. Johns, W. E. and Olson, D. B.: Observations of seasonal exchange through the Strait of Hormuz, *Oceanography*, 11, 58, 1998.
7. Matsuyama, M., Kitade, Y. and Senjyu, T.: Vertical Structure of current and density front in the Strait of Hormuz, *Offshore Environments of the ROPME after the War related Oil-Spill*, 23-34, 1998.
8. Mellor, G. and Yamada, T.: Development of a Turbulence Closure Model for Geophysical Fluid Problems, *Rev. Geophys. Space Phys.*, 20, no. 4, 1982.
9. Pous, S. P., Carton, X., Lazure, P.: Hydrology and circulation in the Strait of Hormuz and the Gulf of Oman result from the GOGP99 Experiment, *J. Geophys. Res.*, 109, 2004.
10. Reynolds, R. M.: Overview of physical oceanographic measurements taken during the Mt. Mitchell Cruise to the ROPME Sea Area, *Mar. Pollution Bull.*, 27, 35-59, 1993.
11. Senjyu, T., Ishimaru, T., Matsuyama, M. and Koike, Y.: High salinity lens from the Strait of Hormuz, *Offshore Environments of the ROPME after the War related Oil-Spill*, 35-48, 1998.
12. Stern, M. E.: Geostrophic fronts, bores, breaking and blocking waves, *J. Fluid Mech.*, 99, 687-704. 1980.
13. Swaters, G. E.: On the baroclinic instability of cold-core coupled density fronts on a sloping continental shelf. *J. Fluid Mech.*, 224, 361–382, 1991.
14. Swift, S. A. and Bower, A. S.: Formation and circulation of dense water in the Persian Gulf, *J. Geophys. Res.*, 108(C1), 2003.